Bound Structures of Novel P3−P1′ β-Strand Mimetic Inhibitors of Thrombin†

Robert St. Charles, John H. Matthews, Erli Zhang, and A. Tulinsky*

Department of Chemistry, Michigan State University, East Lansing, Michigan 48823

Received January 23, 1998

The X-ray crystal structures of four β-strand-templated active site inhibitors of thrombin containing P1′ groups have been determined and refined at about 2.1-Å resolution to crystallographic *R*-values between 0.148 and 0.164. Two of the inhibitors have an α-ketoamide functionality at the scissile bond; the other two have a nonhydrolyzable electrophilic group at the P1′ position. The binding of lysine is compared with that of arginine at the S1 specificity site, while that of D,L-phenylalanine enantiomorphs is compared in the S3 region of thrombin. Four different P1′ moieties bind at the S1′ subsite in three different ways. The binding constants vary between 2.0 μM and 70 pM. The bound structures are used to intercorrelate the various binding constants and also lead to insightful inferences concerning binding at the S1′ site of thrombin.

Introduction

Trypsin-like serine proteases form a large and highly selective family of enzymes in hemostasis/coagulation[1] and in complement activation.[2] Sequencing of these enzymes has shown the presence of a common homologous trypsin-like core with insertions that can modify specificity and selectivity. The insertions can also be generally responsible for interactions with other macromolecules or modules thereof.[3,4] Limited proteolysis is an important biochemical regulatory event that is controlled in vivo by the constant interplay between enzymes and their endogenous inhibitors. Inspection of numerous X-ray crystal structures[3−6] underscores the fact that binding of proteolytic substrates and proteinaceous inhibitors by their cognate enzymes occurs through an extended β-strand motif that is uniformly adopted by the P1−P3 residues of inhibitor/substrate hydrogen bonding with an extended chain conformation of the active site.

A combinatorial approach has been employed in nature for developing an immense array of ligands critical in a wide array of molecular recognition events and biological processes. With regard to peptide and protein ligands, to a first approximation, the 20 amino acid side-chain pharmacophores have been essentially displayed on three priviledged scaffolds: the principal secondary structural elements of α-helices, β-strands, and reverse turns. Proprietary chemistry to build libraries of conformationally constrained/secondary structure mimics has been developed[7−9] and termed SMART libraries for Small Molecular Arrays of Restricted Templates. As part of the program of designing and synthesizing mimetics of the principal secondary structural elements, several templates have been developed and constructed by modular component syntheses that mimic the conformation of a dipeptide constrained within a β-strand.[10,11] Two of these, utilized in the present work, the azabicyclo[4.3.0]nonane and the corresponding diazobicyclo analogue, are shown below. Such secondary structurally constrained mimetics are now being used to routinely generate focused combinatorial libraries as a source for the development of small-molecule therapeutic agents.

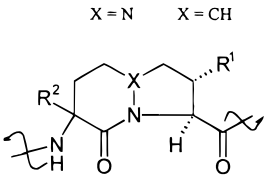

Thrombin is a serine protease that plays an important and diverse role in blood coagulation.[13] Its most prominent functions are the conversion of fibrinogen to fibrin, ultimately resulting in the blood clot and the activation of platelets.[14] The potential for controlled intervention of the coagulation cascade to ameliorate specific disease states has long been recognized and is actively being pursued by pharmaceutical companies. Most of the thrombin−peptide inhibitor complexes studied by X-ray crystallography have been restricted to those that bind to one or the other of the S1−S3 subsites of the active site utilizing a β-strand structure[3,4,6] and nonhydrolyzable tandem inhibitors that bind simultaneously to the active site and the fibrinogen recognition exosite[15−17] or nonpeptidic ones such as DNA aptamers[18] and zinc-mediated small-molecule inhibitors.[19] Much has been revealed by the former work in understanding a wide variety of binding modes and geometries of thrombin but less is known adjacent (C-terminal) to the scissile bond from the S′ subsite binding structures because the corresponding P′ residues have generally been occupied by glycine spacers in the bivalent inhibitors.

One attractive, rational approach toward developing thrombin inhibitors that has been extensively utilized is to uncover good substrates and then convert them to

† Abbreviations: hirugen, sulfated Tyr63-*N*-acetylhirudin 53−64; PPACK, D-Phe-Pro-Arg-chloromethyl ketone; DuP714, boronic acid analogue of PPACK; CVS1347, benzyl-SO_2-Met(O_2)-Pro-Arg(CO)-phenethyl; argatroban, (2*R*,4*R*)-4-methyl-1-[N_α-(3-methyl-1,2,3,4-tetrahydro-8-quinolinylsulfonyl)-L-arginyl]-2-piperidinecarboxylic acid; RWJ 50215, *N*-[[4-[(aminoiminomethyl)amino]-1-[2-(thiazol-2-ylcarbonyl)-ethyl]piperidin-1-ylcarbonyl]butyl]-5-(dimethylamino)naphthalenesulfonamide; RWJ 50353, *N*-methyl-D-Phe-Pro-Arg-2-benzothiazole.

* To whom correspondence should be addressed.

10.1021/jm980052n CCC: $18.00
Published on Web 03/31/1999

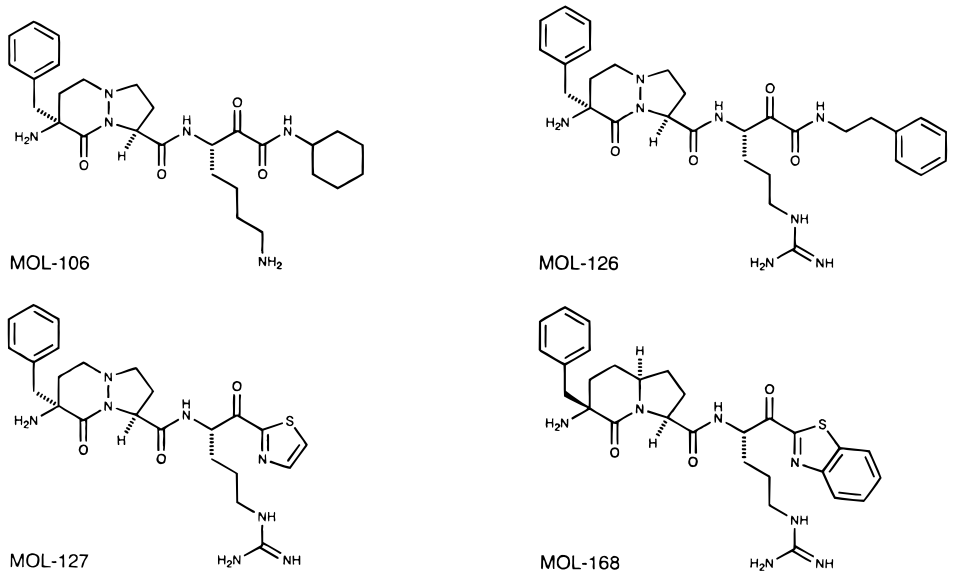

Figure 1. Active site Molecumetics thrombin inhibitors. Note L-Phe at P3 position and deazobicycle at P2 in MOL168.

Table 1. Thrombin Binding Constants of the Molecumetics Inhibitors

	K_i (nM)	MOL(*X*)/MOL126	K_{on} (M^{-1} s^{-1})
MOL106	2000	28000	$\sim 10^5$
MOL126	0.071	1	6.4×10^5
MOL127	2.4	34	$>10^7$
MOL168	10	140	$>10^7$
MOL174[a]	0.65	9	$>10^7$

[a] Structure same as MOL168 but with D-Phe at P3 position.

inhibitors by introducing an electrophilic functional group at the scissile amide bond, which additionally gains enhanced binding with the underutilized and poorly defined S1′ binding subsite of thrombin. The first such example was described in the design of novel heterocyclic inhibitors of the serine protease elastase.[20] The X-ray crystal structure of acetyl-Val-Pro-Val-(2-benzoxazole) bound to elastase revealed no proteolytic cleavage and a new hydrogen-bonding interaction between the benzoxazole nitrogen and His57 of the catalytic triad. A similar interaction has since been found in the thrombin-bound structure of *N*-methyl-D-Phe-Pro-Arg-(2-benzothiazole).[21] The α-ketoamide function is also stable to thrombin cleavage[17,22,23] and provides an additional route to probe the S1′ site of the enzyme. These two nonhydrolyzable features have been combined with β-strand templates to produce highly potent inhibitors of thrombin, some of which have been studied here (Figure 1, Table 1).

We now describe the X-ray crystal structures of four β-strand-templated active site inhibitors containing P1′ groups developed by Molecumetics Ltd. (Bellevue, WA) binding to thrombin (Figure 1).[24] The more potent inhibitory activity of the α-ketoamide derivatives, notwithstanding the considerably faster rate of inactivation of the α-ketothiazole and benzothiazole derivatives (Table 1), makes such compounds more clinically attractive. The MOL174 inhibitor has already been shown to be highly effective in vivo in baboon using the arteriovenous shunt model of thrombosis.[25] The four thrombin-inhibited structures are used to intercorrelate the various binding constants and also lead to insightful inferences concerning binding at the S1′ subsite of thrombin.

Experimental Procedures

Crystals of the hirugen−α-thrombin complex were grown by macroseeding using procedures described previously.[26] Ternary complexes of the active site-directed Molecumetics inhibitors of thrombin (Figure 1) were prepared by soaking hirugen−thrombin crystals in separate storing solutions (28% PEG8000, 0.1 M sodium phosphate buffer (pH 7.3), 0.1 M NaCl) containing the inhibitors. All the inhibitors were initially dissolved in 5% methanol prior to their addition to the storing solution. The concentration of inhibitor in the storing solution was incrementally increased over a 4−5-day period to a final concentration of 5−7 mM. All the ternary complex crystals were isomorphous with native crystals of hirugen−thrombin[26] (Table 2 in Supporting Information).

Three X-ray intensity data sets (MOL126, MOL127, MOL168) were measured with a R-AXIS II imaging plate detector, while MOL106 data were collected with a Siemens X-1000 multiwire detector. Both detectors were coupled to a Rigaku RU200 rotating anode X-ray generator using a fine focus filament (0.3 × 3.0 mm) and operating at a power setting of 5 kW (50 kV, 100 mA). Factors and statistics pertinent to the intensity data collections and processing are summarized in Table 2 (Supporting Information). Structure analysis of the ternary thrombin complexes began with a rigid body rotation−translation refinement using the coordinates of the hirugen−thrombin structure (PDB 1HAH),[29] less hirugen and water molecules. The hirugen and the active site inhibitor were located in early 2.8-Å resolution ($2|F_o| - |F_c|$) and ($|F_o| - |F_c|$) electron density maps and included into refinement calculations. Initial coordinates and stereochemical restraints for the nonprotein portions of the inhibitors were either obtained from the Cambridge Structural Database or prepared using the Builder module of Insight II (Molecular Simulations, Inc.). The complete structures were refined with the program PROLSQ.[30] Water molecules and two Na^+ ions[31,32] were introduced at 2.5-Å resolution. In the final stages of refinement, a Bragg angle dependent $\sigma(|F_o|)$ was used to weight the diffraction pattern based on $\langle|F|\rangle$ in different 2θ shells. The ranges of the least-squares restraints and deviations from ideal geometry are listed in Table 3 (Supporting Information), while some individual refinement indicator parameters are given in Table 4 (Supporting Information). The coordinates of the ternary complexes have been deposited in the Brookhaven Protein Data Bank (MOL106, 1A46; MOL126, 1A5G; MOL127, 1A61; MOL168, 1B5G).

Results and Discussion

Thrombin Structure. Electron density was well-defined for most of the A-chain and B-chain of thrombin

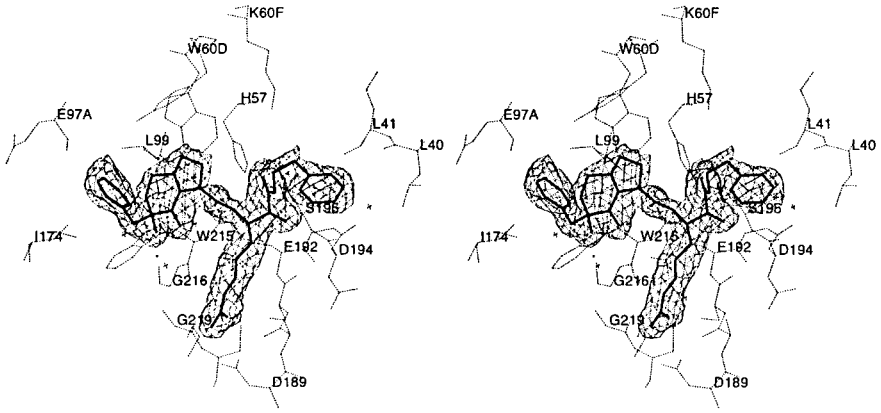

Figure 2. Stereoview of omit map of MOL126. Contoured at 1σ; thrombin residues dotted; water molecules indicated by crosses.

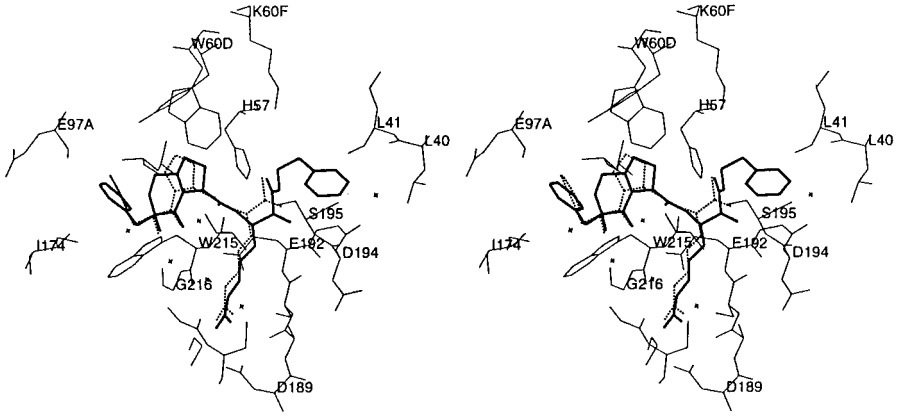

Figure 3. Stereoview of PPACK superposed on MOL126−thrombin. MOL126 in bold; PPACK dotted; thrombin (thin lines) and water structure as in Figure 2.

in each of the four thrombin−inhibitor complexes. Those regions in the electron density maps which were weak corresponded to several residues at the termini of the A-chain, within the autolysis loop, and at the C-terminus of the B-chain, regions typically found to be disordered in other isomorphous thrombin complexes.[26,29] The hirugen molecule had moderate to good density for residues Asp55 to Leu64 in all the complexes. The final thrombin models in the four crystal structures are very similar, with an average rms difference in optimally superposed C_α coordinates of about 0.23 Å. The largest average rms difference is 0.26 Å, between the MOL106 and MOL168 complexes, and the smallest is 0.19 Å, between the MOL126 and MOL127 complexes.

Inhibitor Interactions with Thrombin. Electron density was well-defined for each MOL inhibitor in the final ($2|F_o| - |F_c|$) maps (Figure 2), except for the L-phenylalanyl group of MOL168 (discussed below). All the inhibitors bind to the active site of thrombin in a fashion similar to PPACK[33] (Figure 3). As the bicyclic and phenylalanyl group of each inhibitor approximate the extended conformation of PPACK in PPACK-bound thrombin, most of the P1−P3 interactions observed in the latter are common to the MOL inhibitor complexes (Figures 3 and 4). As expected, antiparallel β-strand hydrogen-bonded interactions are observed in all cases between the bicyclic β-strand-templated carbonyl oxygen and its amino nitrogen atom and the Ser214−Gly216 main chain segment of thrombin (Table 5).

The positively charged side chain of the P1 residue of each inhibitor is bound within the primary specificity pocket of thrombin making a hydrogen-bonded salt bridge[34] with the acidic side chain of Asp189 and other hydrogen bonds to water molecules (Figures 5−7). The bicyclic group of each inhibitor occupies the apolar S2 and part of the S3 region of the active site making hydrophobic contacts with the side chains from His57, Tyr60A, Trp60D, and Trp215 (Figures 5−7). In superpositions with other P2 proline-containing inhibitors and substrates complexed with thrombin, the five-membered ring of the bicyclic ring overlaps closely that region occupied by the proline ring in these molecules[15−17,35−38] (Figure 3). As in PPACK, the D-phenylalanyl group of MOL106, MOL126, and MOL127 is buried within the aryl D-enantionmorphic S3 binding site and interacts with side chains from Leu99, Ile174, and Trp215 (Figures 3−6), while the L-phenylalanyl of MOL168 occupies the aspartate L-enantiomorphic S3 subsite as observed with the Leu-Asp-Pro-Arg sequence of the thrombin platelet receptor peptide fragment bound to thrombin[35] (Figure 7). The polar interactions between the MOL inhibitors and thrombin are summarized in Table 5.

MOL106 and MOL126 Structures. The N-terminal P2−P3 residues of MOL106 and MOL126 are identical and similar to those of PPACK, but with more bulk and rigidity introduced by a two-atom link between what would be CA of the D-phenylalanyl and CD of the proline of PPACK, giving a heterobicyclic system of fused five- and six-membered rings (Figure 1). This part of both inhibitors interacts with thrombin in a manner similar to the prolyl and D-phenylalanyl residues of PPACK[33]

Table 5. Polar Active Site Interactions of the Inhibitors[a]

	interactions, inhibitor	distances (Å)				type
		MOL106	MOL126	MOL127	MOL168	
Bic370N3	Gly216O	2.7	2.7	2.4	3.0	H-bond
Bic370O1	Gly216N	3.1	3.2	2.8	3.2	H-bond
Bic370N3	O_w484[b]	3.3	2.8			H-bond
Bic370O2	O_w484	2.9	2.5		2.8	H-bond
Bic370N3	O_w535		2.8			H-bond
Arg372N	Ser214O	3.3	3.2	3.3	3.2	H-bond
Arg372NH1	Asp189OD2		2.9	2.6	3.1	H-bond
Arg372NH1	O_w422		3.1	3.1	3.1	H-bond
Arg372NH2	Asp189OD1	3.1 (NZ)	2.6	2.4	2.6	H-bond
Arg372NH2	Gly219O	2.7 (NZ)	2.8	3.0	2.7	H-bond
Arg372NH2	Ala190O	3.0 (NZ)				H-bond
Arg372NE	O_w418		2.9	3.0	2.9	H-bond
Arg372C	Ser195OG	1.8	1.8	1.8	1.8	transition-state bond
Arg372O	Gly193N	3.0	2.7	3.1	2.9	H-bond
Arg372O	Gly195N	3.0	2.9	2.5	2.6	H-bond
LysNZ	O_w425	2.8				H-bond
Cyc374O1	His57NE2	2.7				H-bond
Eoa374O1	His57NE2		2.7			H-bond
Thz374N1	His57NE2			2.7		H-bond
Thz374S1	O_w528				2.8	possible H-bond
Bnz374N1	His57NE2				2.7	H-bond
O_w418	Glu192OE2		2.5	2.4 (OE1)	3.0	H-bond
O_w418	Gly219O		2.7	2.8	3.0	H-bond
O_w422	Eoa227O		3.2	3.1	2.9	H-bond
O_w425[c]	Asp189OD2	2.6				H-bond
O_w484	Glu192OE2	2.6	2.7		2.4 (OE1)	H-bond
O_w528[d]	Glu192OE1				3.0	H-bond

[a] Bic, bicyclic P2 residue; Cyc, cyclohexyl; Eoa, phenethyl; Thz, 2-thiazole; Bnz, 2-benzothiazole. [b] O_w are water molecules in MOL126 complex and corresponding equivalents of other complexes. [c] O_w425 only present in MOL106 complex. [d] O_w528 only present in MOL168 complex.

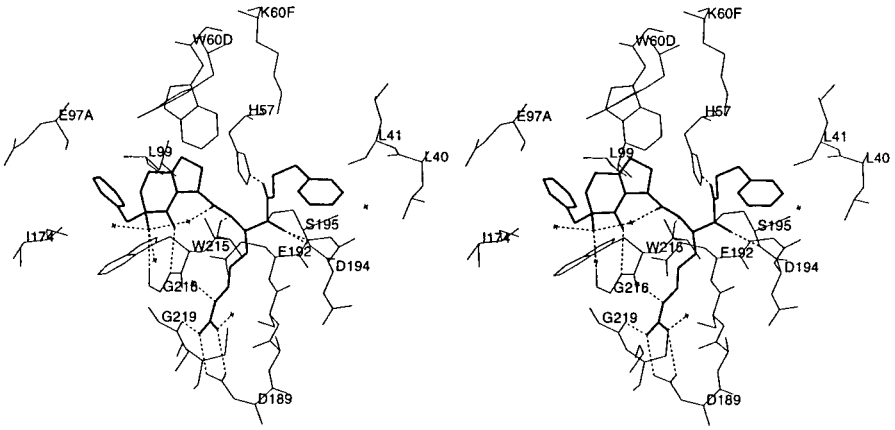

Figure 4. Stereoview of hydrogen bonding in MOL126−thrombin structure. MOL126 in bold; thrombin and water structure as in Figures 2 and 3; hydrogen bonds broken.

(Figures 3−6). The N and O atoms equivalent to those of D-phenylalanyl in PPACK form antiparallel β-strand hydrogen bonds with Gly216 (Figure 4). The D-phenylalanyl group binds in an aryl nonpolar cavity surrounded by Leu99, Ile174, and Trp 215. The bicycle occupies a larger space bounded by Tyr60A and Trp60D from one side, with the five-membered heterocycle occupying about the same position as the proline of PPACK (Figure 3). In both MOL inhibitor structures, the second carbonyl oxygen (O2) of the bicyclic group is linked to the side chain of Glu192 by a water molecule (Figures 3 and 4).

The P1 residues of these two inhibitor molecules form ion pairs with Asp189. In the MOL126 structure, a doubly hydrogen-bonded salt bridge occurs between the P1 arginine side chain and the carboxylate of Asp189 in a manner common to arginine−thrombin inhibitor complexes.[32] The P1 residue of MOL106 is a lysine, instead of arginine. This partially accounts for the weaker inhibitory activity of MOL106 for thrombin (K_i about 2 μM compared to 0.08 nM for MOL126). The lysine NZ atom makes a hydrogen bond contact with Asp189OD1 (3.1 Å). This differs from the thrombin complex of the lysine analogue of DuP714,[36] where a water molecule bridges the lysine amine and the Asp189 carboxylate with no direct contact between the two side chains (NH_2−Asp189OD2 = 3.5 Å). A direct ion pair, however, was observed in a molecule related to DuP714 with a P1 homolysine (one additional methylene group in the side chain)[36] and the inhibitor L-372,912 bound to thrombin, which has a cyclohexylamine group at the P1 position.[39] In the MOL106 structure, the NZ atom occupies a position essentially equivalent to that of one of the NH groups of arginine-based inhibitors of thrombin. A water molecule (O_w425) in MOL106 near the other arginine NH position connects lysine NZ with OD2

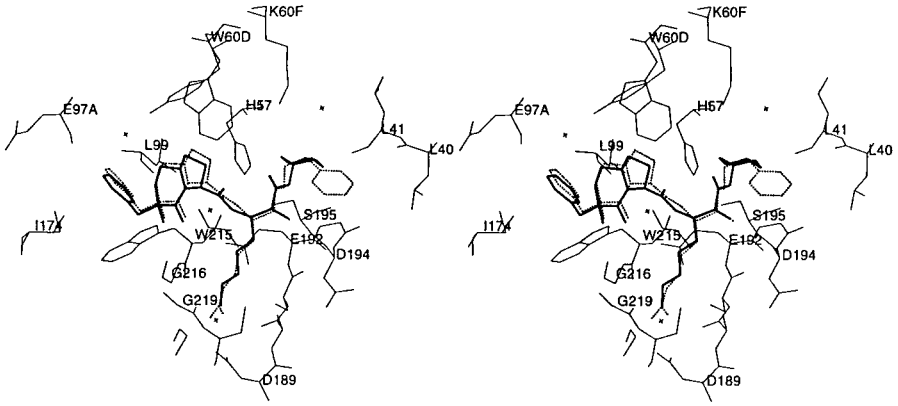

Figure 5. Stereoview of MOL126 (dotted) superposed on MOL106−thrombin (bold).

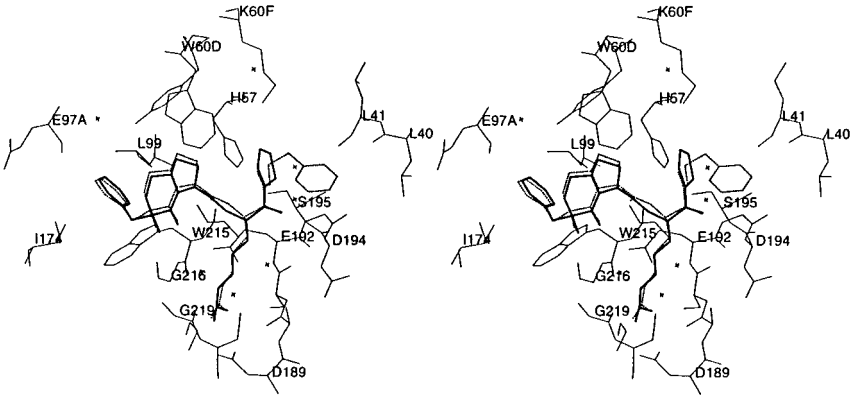

Figure 6. Stereoview of MOL126 (dotted) superposed on MOL127−thrombin (bold).

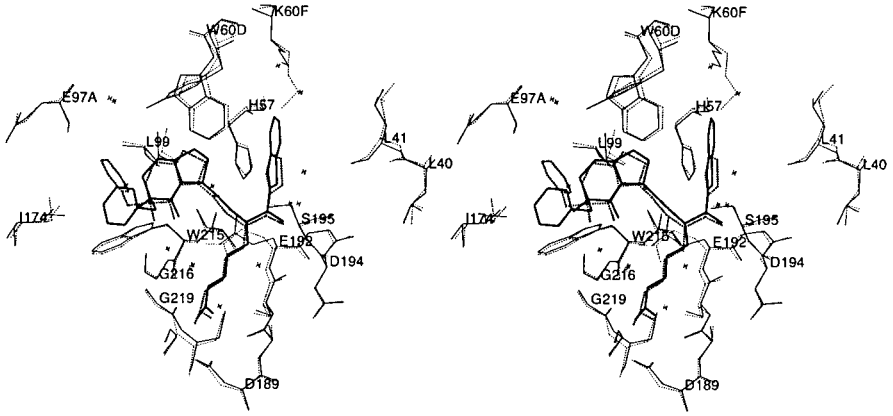

Figure 7. Stereoview of MOL127 thrombin (dotted) superposed on MOL168−thrombin (bold and thin lines).

of Asp189. The lysine NZ participates in other interactions observed in the arginine inhibitors including a hydrogen bond to Gly219O[32] and a O_w425-O_w384-mediated link to Phe 227O.

The α-ketoamide groups of the MOL106 and MOL126 inhibitors bind to thrombin in a manner that resembles the hemiketal tetrahedral transition-state species proposed for peptide hydrolysis by serine proteases.[17,31,37] In both thrombin complexes, Ser195OG forms a hemiketal intermediate with the carbonyl carbon (∼1.8 Å) of the P1 residues of the inhibitors. The additional α-ketoamide carbonyl of MOL106, MOL126, and other such inhibitors[17,37] obviates hydrolysis of the scissile peptide bond. The O−C−C−O torsion angle of the α-ketoamide moiety is 145° in MOL106 and 133° in MOL126 (compared to 131° in cyclotheonamide A[37] and 116° in the more restrained bivalent inhibitor CVS995[17]). In both MOL structures, the keto oxygen hydrogen bonds to Gly193N and Ser195N of the oxyanion hole and the amide carbonyl forms a hydrogen bond with His57NE2 (Table 5). These interactions are also observed in the structure of thrombin complexed with cyclotheonamide A[37] and CVS995[17] and the trypsin and thrombin structures inhibited with *p*-amidinophenylpyruvate.[40,41] However, the interaction pattern is surprisingly reversed with thrombin and the α-ketoacid hydrolysis product of the P1′ phenethyl inhibitor CVS1347.[38] In that structure, an oxygen of the carboxylate group binds to the oxyanion hole and the keto oxygen makes the hydrogen bond with His57. Because of formation of the hemiketal intermediate, a larger negative charge would be expected on the keto oxygen atom than the amide oxygen in MOL106 and MOL126. In CVS1347, however, the carboxylate is negatively charged. This apparent

preference of the oxyanion hole for anionic groups is consistent with the suggested role of the loop in stabilizing the negatively charged oxygen of the tetrahedral intermediate in protease cleavage. The hydrogen bonds in the oxyanion hole may be weaker in MOL106 than in MOL126 and CVS1347 (both N−O distances are 3.0 Å in MOL106 and are about 2.8 Å in MOL126 and CVS1347).

In MOL106 and MOL126 the segment of the inhibitor C-terminal to the scissile bond (P1′) is hydrophobic and occupies the so-called "southern" region[33] of the S1′ and S2′ subsites (Figure 5). The cyclohexyl group of MOL106 is surrounded by side chains from Cys42, Cys58, His 57, Trp60D, and Lys60F and the main chain of Cys42, Gly43, Glu192, and Gly193 (Figure 5). This general region was shown to be the S1′ site in the structures of thrombin complexes with the noncleavable divalent inhibitors hirulog-3,[15] hirutonin 2,[16] hirutonin 6,[16] and CVS995[17] and with a singly substituted P1′ active site inhibitor RWJ 50353.[21] The cyclohexane ring, in a chair conformation, is linked to the ketoamide axially to the equatorial plane of the ring, packs within van der Waals contacts with the N and CA atoms of Gly193, and makes closest contacts with the side chain of Trp60D and the carbonyl oxygen of Leu41. The phenethyl group of MOL126 binds similarly, but because its linker is two bond lengths longer, the ring extends farther "south" into the S1′ and possibly into some of the S2′ subsite (Figure 5) toward the side chain of Gln151, also interacting closely with Gly193 and displacing a water molecule found in this region of the PPACK and hirugen structures of thrombin (Figure 3). Interactions with the Glu192−Gly193 main chain are most significant, with the phenyl ring packing flat against the peptide plane of the two residues (Figure 3). The phenethyl also impinges on the Leu41 main chain making a good van der Waals contact with Leu41O. These differences in the P1′ interactions of MOL106 and MOL126, together with the differences in the binding of lysine (MOL106) and arginine (MOL126) in the S1 specificity site, are the major factors determining the difference in their inhibitory activity.

Binding of the P1′ residues of both of these inhibitors within the "southern" S1′ region does not disturb the side chain of Lys60F from extending into the subsite similar to the argatroban-like RWJ 50215 inhibitor of thrombin in which a small keto-2-thiazole group is present.[21] This inhibitor binds to thrombin with the ketothiazole group occupying the "northeast" corner of the cavity. The P1′ benzothiazole PPACK analogue (RWJ 50353) has the thrombin-bound P1′ benzothiazole pointing "north" in the S1′ site, which causes the conformation of Lys60F to change in order to avoid collision.[21] A similar change is observed with MOL168 binding to thrombin (Figure 7).

MOL127 and MOL168 Structures. Electron density for these two inhibitors was also well-defined but with that of the L-phenylalanyl group of MOL168 being only moderately so. Although density for the N-terminal group was weak, it was nonetheless sufficient to unambiguously identify the position of the phenyl ring around its CA−CB bond (Figure 7). The Ser195OG atom of thrombin again forms a hemiketal intermediate with the carbonyl carbon of the P1 arginine of both MOL127 and MOL168. The geometry of the substituents around the carbonyl carbon is distorted tetrahedral, with the carbonyl oxygen occupying the oxyanion hole making hydrogen bonds with Gly193N and Ser195N (Table 5). The arginyl side chain in both inhibitors makes a doubly hydrogen-bonded salt bridge with carboxylate side chain of Asp189 as in MOL126 and nearly all other thrombin inhibitors with an arginine residue in the P1 position[32] (Figures 2 and 3). The NE atom of each arginine makes a hydrogen bond with a well-ordered water molecule located between it and the side chain of Glu192 (Table 5). This water is conserved in many other tripeptide active site inhibitors of thrombin containing a P1 arginine.[32,36] Most of the several other ordered water molecules within the active site are common to both inhibitor structures and are also present in PPACK thrombin and other anginyl inhibitor structures (Table 5). The methine carbon substitution of a nitrogen atom at one bridge of the bicyclic P2 group of MOL168 (Figure 1) does not appear to have any significant effect on either the structure or the binding ability of the inhibitor (Figure 7). While the D-phenylalanyl group of MOL106, MOL126, and MOL127 binds to the D-enantiomorphic subsite in a manner nearly identical to PPACK, the L-conformation of the phenyl group of MOL168 is bound in the L-enantiomorphic S3 binding site of thrombin, similar to the aspartic acid residue of the thrombin platelet receptor peptide fragment of Leu-Asp-Pro-Arg bound to thrombin,[35] and is located in a more solvated region near Glu217 (Figure 7). The 2-thiazole group of MOL127 and the 2-benzothiazole of MOL168 bind in the S1′ region of thrombin somewhat similar to the cyclohexyl of MOL106 but not the phenethyl group of MOL126 (Figures 5−7). Both the thiazole and benzothiazole rings are practically in the same orientation and are surrounded by side chains from Cys42, His57, Tyr60A, Trp60D, and Lys60F. The thiazole ring of both inhibitors is closest to the side chain of His57 (Figure 7). In both complexes, the thiazole nitrogen is pointed toward His57 and makes a hydrogen bond with the NE imidazole ring nitrogen atom.

A similar orientation was observed for the benzothiazole ring of the inhibitor RWJ 50353 complexed with thrombin.[21] The thiazole sulfur atom of both inhibitors points toward Glu192 and possibly interacts (3.7 Å) with the amide nitrogen of Gly193. The larger benzothiazole of MOL168 extends "northward" in the S1′ subsite to interact more significantly with 60-insertion loop side chains of the Tyr60A, Trp60D, and Lys60F of thrombin. Its closest contact is with the indole ring of Trp60D, which stacks nearly perpendicular (on edge) to the plane of the benzothiazole group (Figure 7). In addition, "northward" extension of the benzothiazole in the S1′ subsite forces the side chain of Lys60F to move in a direction away from the catalytic center, with its distal atoms being displaced an average of 0.8 Å when compared with those in the hirugen−thrombin structure[29] or those of MOL106, MOL126, and MOL127. The movement does not occur in the MOL127−thrombin complex due to the smaller thiazole ring in the S1′ position and lack of a "northward" excursion of the cyclohexyl and phenethyl groups in MOL106 and MOL126 (Figures 5 and 6). As in the hirugen−thrombin structure, the NZ of Lys60F makes a hydrogen bond

with His57O in these structures, an interaction not observed in the MOL168 complex. The hydrogen bond is conserved in other thrombin models including those crystal structures of thrombin complexed with non-cleavable substrate analogues in which the S1′ site is occupied by glycine. Since the K_i of MOL168 is 10 nM compared to 2.4 nM for MOL127, it would seem that the benzothiazole must make up much of the lost binding affinity for the presence of L-phenylalanyl in the P3 position of MOL168, so the effect of the benzothiazole on Lys60F appears to be of minimal importance to binding.

Concluding Remarks

The MOL126 inhibitor has by far the best specificity for thrombin, followed by MOL127, MOL168, and MOL106 in that decreasing order (Table 1). The K_i of 80 pM of MOL126 suggests it is as potent an inhibitor of thrombin as can be expected from a four-peptide unit. In comparison, MOL106 is also an α-ketoamide, but about 28 000 times less effective (Table 1), having lysine at the P1 position instead of arginine and cyclohexyl instead of phenethyl at P1′. The K_i of DuP714 is 0.04 nM, while that of its lysine analogue is only 2.4 nM,[36] so the effect of the lysine substitution is a loss of about 2 orders of magnitude in inhibitory ability. If the same applies between MOL126 and MOL106, then the difference at the P1′ position must also account for about a factor of 100 in binding to thrombin. The remaining affinity is very likely related to the more extended contacts possible with the phenethyl group compared to cyclohexyl and the aromaticity of the former compared to the highly hydrophobic nature of the cyclohexyl group.

Somewhat similar arguments apply to the difference between the binding capability of MOL126 and MOL127, although here the scissile bond functionality is different in addition to the P1′ position (Figures 1 and 6). The MOL126 inhibitor is only about 1 order of magnitude better than MOL127 (Table 1). Much of the gain in binding from the P1′ position of MOL127 compared to MOL126 must reside in the hydrogen bond the thiazole makes with His57NE and the interaction of the ring sulfur atom with Gly193N, interactions not possible with the phenethyl group of MOL126. When MOL168 is also included in the comparison, a factor of about 5 in binding with respect to MOL127 is somewhat unexpected considering that the favorable binding component from the D-phenylalanine S3 subsite is lost with L-phenylalanyl at P3 and the steric clash between its benzothiazole and Lys60F. As with the thiazole of MOL127, however, the nitrogen and sulfur interactions of the benzothiazole of MOL168 apparently compensate satisfactorily for the 15-fold loss of affinity certainly introduced by the aromatic L-enantiomorph in the P3 position (Table 1). It is clear from the MOL168 structure that the L-phenylalanine is located in solvent space and is not a very important component to the binding of the inhibitor (Figure 7). This is also evidenced by the average *B*-value of the L-enantiomorphic P3 group (40 Å^2) compared to that of thrombin (28 Å^2).

The S1′ subsite of thrombin generally accommodates smaller amino acid side chains as observed from the P1′ residues of a number of natural substrates.[15] These residues include glycine, alanine, serine, and threonine; however, they also include Val20 of fibrinogen A, Leu13 of protein C, and Ile153 and Ile370 of factor VII and factor XI, respectively, and again the P1′ position displays the penchant of thrombin to tolerate imprecision.[4,6] The ability to bind leucine and isoleucine in S1′ is in agreement with the MOL168 structure and its relatively large P1′ benzothiazole group. The S1′ site therefore is capable of harboring moderately bulky side groups even though it appears to prefer smaller ones.[15] The latter may be related to the main chain path through the S1′ site, which shows a fairly sharp turn in the case of glycine in nonhydrolyzable bivalent inhibitors causing a strained conformational angle not allowed for non-glycyl amino acids.[15,17] The smaller side group preference may thus be actually connected with the ability of the main chain to attain a strained configuration for catalysis, which appears not to rule out bulkier P1′ groups per se, like leucine and isoleucine. The phenethyl of MOL126 mimics the P1′ turn of hirulog 3[15] and CVS995[17] (Figure 5). The ability to do so is due to the longer linker to the phenyl group which, in combination with the more abundant protein interactions of the latter, produces, by any standards, a very potent thrombin inhibitor.

Acknowledgment. This work was supported by NIH Grant HL 43229 and in part by Molecumetics Ltd.

Supporting Information Available: Tables 2−4 contain factors describing X-ray diffraction quality, deviations from idealized geometry, and refinement indicator parameters, respectively. This information is available free of charge via the Internet at http://pubs.acs.org.

References

(1) Davie, E. W.; Fujikawa, K.; Kisiel, W. The Coagulation Cascade: Initiation, Maintenance, and Regulation. *Biochemistry* **1991**, *30*, 10363−10370.
(2) Muller-Eberhard, H. J. Complement. *Annu. Rev. Biochem.* **1975**, *44*, 697−724.
(3) Stubbs, M. T.; Bode, W. A Player of Many Parts: The Spotlight Falls on Thrombin's Structure. *Thromb. Res.* **1993**, *69*, 1−58.
(4) Tulinsky, A. Molecular Interactions of Thrombin. *Sem. Thromb. Hemostas.* **1996**, *22*, 117−124
(5) Bode, W.; Huber, R. Natural Protein Proteinase Inhibitors and Their Interaction with Proteinases. *Eur. J. Biochem.* **1992**, *204*, 433−451.
(6) Tulinsky, A.; Qiu, X. Active Site and Exosite Binding of α-Thrombin. *Blood Coag. Fibrin.* **1993**, *4*, 305−312.
(7) Kahn, M.; Wilke, S.; Chen, B.; Fujita, K. Nonpeptide Mimetics of *β*-Turns: A Facile Oxidation Intramolecular Cycloaddition of an Azodicarbonyl System. *J. Am. Chem. Soc.* **1988**, *110*, 1638−1639.
(8) Nakanishi, H.; Chrusciel, R. A.; Shen, R.; Bertenshaw, S.; Johnson, M. E.; Rydel, T. J.; Tulinsky, A.; Kahn, M. Peptide Mimetics of the Thrombin-Bound Structure of Fibrinopeptide A. *Proc. Natl. Acad. Sci. U.S.A.* **1992**, *89*, 1705−1709.
(9) Wu, T.-P.; Yee, V.; Tulinsky, A.; Chrusciel, R. A.; Nakanishi, H.; Shen, R.; Priebe, C.; Kahn, M. The Structure of a Designed Peptidomimetic Inhibitor Complex of α-Thrombin. *Protein Eng.* **1993**, *6*, 471−478.
(10) Eguchi, M.; Boatman, P. D.; Ogbu, C. O.; Nakanishi, H.; Bolong, C.; Lee, M. S.; Kahn, M. Dipeptide Mimetics for Thrombin Substrates and Inhibitors. 212th American Chemical Society National Meeting, Orlando, FL, 1996; MEDI 125.
(11) Kim, H.-O.; Kahn, M. Short Synthesis of (3S,6S,9S)-2-Oxo-3-(N-Boc-amino)-1-azabicyclo[4.3.0]nonane-9-carboxylic Acid Methyl Ester: Tandem Cyclization Protocol. *Tetrahedron Lett.* **1997**, *38*, 6483−6484.
(12) Eguchi, M.; Kim, H.-O.; Gardner, B. S.; Boatman, P. D.; Lee, M. S.; Nakanishi, H.; Kahn, M. Synthesis of Dipeptide Secondary Structure Mimetics. *Proc. 15th Am. Pept. Symposium*; Kluwer Academic Publishers: Dordrecht, The Netherlands, 1998.
(13) Mann, K. G. The Assembly of Blood Clotting Complexes on Membranes. *Trends Biochem. Sci.* **1987**, *12*, 229−233.

(14) Blomback, B.; Blomback, M.; Hessel, B.; Iwanaga, S. Structures of N−Terminal Fragments of Fibrinogen and Specificity of Thrombin. *Nature* **1967**, *215*, 1445−1448.
(15) Qiu, X.; Padmanabhan, K. P.; Carperos, V. E.; Tulinsky, A.; Kline, T.; Maraganore, J. M.; Fenton, J. W. Structure of the Hirulog 3-Thrombin Complex and Nature of the S1′ Subsites of Substrates and Inhibitors. *Biochemistry* **1992**, *31*, 11689−11697.
(16) Zdanov, A.; Wu, S.; DiMaio, J.; Konishi, Y.; Li, Y.; Wu, X.; Edwards, B. F. P.; Martin, P. D.; Cygler, M. Crystal Structure of the Complex of Human α-Thrombin and Nonhydrolyzable Bifunctional Inhibitors, Hirutonin-2 and Hirutonin-6. *Proteins* **1993**, *17*, 252−265.
(17) Krishnan, R. A.; Tulinsky, A.; Vlasuk, G. P.; Pearson, D.; Vallar, P.; Bergum, P.; Brunck, T. K.; Ripka, W. C. Synthesis, Structures, and Structure−Activity Relationships of Divalent Thrombin Inhibitors Containing an α-Ketoamide Transition State Mimetic. *Protein Sci.* **1996**, *5*, 422−433.
(18) Padmanabhan, K.; Tulinsky, A. An Ambiguous Structure of a DNA 15-mer Thrombin Complex. *Acta Crystallogr.* **1996**, *B52*, 272−282.
(19) Katz, B. A.; Clark, J. M.; Finer-Moore, J. S.; Jenkins, T. E.; Johnson, C. R.; Ross, M. J.; Luong, C.; Moore, W. R.; Stroud, R. M. Design of Potent Selective Zinc-Mediated Serine Protease Inhibitors. *Nature* **1998**, *391*, 608−612.
(20) Edwards, P. D.; Meyer, E. F., Jr.; Vijayalakshmi, J.; Tuthill, P. A.; Andisik, D. A.; Gomes, B.; Strimpler, A. Design, Synthesis, and Kinetic Evaluation of a Unique Class of Elastase Inhibitors, the Peptidyl α-Ketobenzoxazoles, and the X-ray Crystal Structure of the Covalent Complex Between Porcine Pancreatic Elastase and Ac-Val-Pro-Val-2-Benzoxazole. *J. Am. Chem. Soc.* **1992**, *114*, 1854−1863.
(21) Matthews, J. H.; Krishnan, R.; Costanzo, M. J.; Maryanoff, B. E.; Tulinsky, A. Crystal Structures of Thrombin with Thiazole-Containing Inhibitors: Probes of the S1′ Binding Site. *Biophys. J.* **1996**, *71*, 2830−2839.
(22) Powers, J. C.; Harper, J. W. Inhibitors of Serine Proteinases. In *Proteinase Inhibitors*; Barrett, A. J., Salvesen, G., Eds.; Elsevier Science Publishers BV: The Netherlands, 1986; pp 55−152.
(23) Maryanoff, B. E.; Qiu, X.; Padmanabhan, K. P.; Tulinsky, A.; Almond, H. R., Jr.; Andrade-Gordon, P.; Greco, M. N.; Kauffman, J. A.; Nicolaou, K. C.; Liu, A.; Brungs, P. H.; Fusetani, N. Molecular Basis for the Inhibition of Human α-Thrombin by the Macrocyclic Peptide Cyclotheonamide A. *Proc. Natl. Acad. Sci. U.S.A.* **1993**, *90*, 8048−8052.
(24) Details of design and synthesis appear in the preceding paper; see: Boatman, P. D.; et al. Secondary Structure Peptide Mimetics: Design, Synthesis, and Evaluation of *β*-Strand Mimetic Thrombin Inhibitors. *J. Med. Chem.* **1999**, *42*, 1367−1375.
(25) Harker, L.; Kahn, M. Unpublished results.
(26) Skrzypczk-Jankun, E.; Carperos, V. E.; Ravichandran, K. G.; Tulinsky, A.; Westbrook, M.; Maraganore, J. M. Structure of the Hirugen and Hirulog 1 Complexes of α-Thrombin. *J. Mol. Biol.* **1991**, *221*, 1379−1393.
(27) Howard, A. J.; Gilliland, G. L.; Finzel, B. C.; Poulos, T. L.; Ohlendorf, D. H.; Salemme, F. R. The Use of An Imaging Proportional Counter in Macromolecular Crystallography. *J. Appl. Crystallogr.* **1987**, *20*, 383−387.
(28) Higashi, T. Auto-indexing of Oscillation Images. *J. Appl. Crystallogr.* **1990**, *23*, 253−257.
(29) Vijayalakshmi, J.; Padmanabhan, K. P.; Mann, K. G.; Tulinsky, A. The Isomorphous Structures of Prethrombin 2, Hirugen, and PPACK−Thrombin: Changes Accompanying Activation and Exosite Binding to Thrombin. *Protein Sci.* **1994**, *3*, 2254−2271.
(30) Hendrickson, W. A. Stereochemically Restrained Refinement of Macromolecular Structure. *Methods Enzymol.* **1985**, *115*, 252−270.
(31) DiCera, E.; Guinto, E. R.; Vindigni, A.; Dang, Q. D.; Ayala, Y. M.; Meng, W.; Tulinsky, A. The Na^+ Binding Site of Thrombin. *J. Biol. Chem.* **1995**, *270*, 22089−22092.
(32) Zhang, E.; Tulinsky, A. The Molecular Environment of the Na^+ Binding Site of Thrombin. *Biophys. Chem.* **1997**, *63*, 185−200.
(33) Bode, W.; Turk, D.; Karshikov, A. The Refined 1.9-Å X-ray Crystal Structure of D-Phe-Pro-Arg-Chloromethyl Ketone-Inhibited Human α-Thrombin: Structure Analysis, Overall Structure, Electrostatic Properties, Detailed Active-Site Geometry, and Structure−Function Relationships. *Protein Sci.* **1992**, *1*, 426−471.
(34) For a description of hydrogen bonds between charged side chains in proteins, see: *Hydrogen Bonding in Biological Structures*; Jeffrey, G. A., Saenger, W., Eds.; Springer-Verlag: New York, 1991; pp 371−372.
(35) Mathews, I. I.; Padmanabhan, K. P.; Ganesh, V.; Tulinsky, A.; Ishii, M.; Chen, J.; Turck, C. W.; Coughlin, S. R.; Fenton, J. W., II. Crystallographic Structures of Thrombin Complexed with Thrombin Receptor Peptides: Existence of Expected and Novel Binding Modes. *Biochemistry* **1994**, *33*, 3266−3279.
(36) Weber, P. C.; Lee, S. L.; Lewandowski, F. A.; Schadt, M. C.; Chang, C. H.; Kettner, C. A. Kinetic and Crytallographic Studies of Thrombin with Ac-(D)Phe-Pro-Boro-Arg-OH and Its Lysine, Amidine, Homolysine, and Ornithine Analogues. *Biochemistry* **1995**, *34*, 3750−3757.
(37) Ganesh, V.; Lee, A. Y.; Clardy, J.; Tulinsky, A. Comparison of the Structures of the Cyclotheonamide A Complexes of Human α-Thrombin and Bovine *β*-Trypsin. *Protein Sci.* **1996**, *5*, 825−835.
(38) Hakansson, K.; Tulinsky, A.; Abelman, M. M.; Miller, T. A.; Vlasuk, G. P.; Bergum, P. W.; Lim-Wilby, M. S. L.; Brunck, T. K. Crystallographic Structures of a Peptidyl Keto Acid Inhibitor and Human α-Thrombin. *Bioorg. Med. Chem.* **1995**, *3*, 1009−1017.
(39) Lyle, T. A.; Chen, Z.; Appleby, S. D.; Freidinger, R. M.; Gardell, S. J.; Lewis, S. D.; Li, Y.; Lyle, E. A.; Lynch, J. J.; Mulichak, A. M.; Ng, A. S.; Naylor-Olsen, A. M.; Sanders, W. M. Synthesis, Evaluation and Crystallographic Analysis of L-371,912. *Bioorg. Med. Chem. Lett.* **1997**, *7*, 67−72.
(40) Walter, J.; Bode, W. The X-ray Crystal Structure Analysis of the Refined Complex Formed by Bovine Trypsin and *ρ*-Amidinophenylpyruvate at 1.4 Å Resolution. *Z. Physiol. Chem.* **1983**, *364*, 949−959.
(41) Chen, Z.; Li, Y.; Mulichak, A. M.; Lewis, S. D.; Shafer, J. A. Crystal Structure of Human α-Thrombin Complexed with Hirugen and *ρ*-Amidinophenylpyruvate at 1.6 Å Resolution. *Arch. Biochem. Biophys.* **1995**, *322*, 198−203.

JM980052N